

# Magnetism, Structure and Superconductivity in $\text{Ce}_2\text{RhIn}_8$

M. Nicklas, V. A. Sidorov,<sup>\*</sup> H. A. Borges,<sup>†</sup> P. G. Pagliuso, C. Petrovic,<sup>‡</sup> Z. Fisk,<sup>§</sup> J. L. Sarrao, and J. D. Thompson  
*Los Alamos National Laboratory, Los Alamos, NM 87545*

(Dated: December 2, 2024)

$\text{Ce}_2\text{RhIn}_8$  is a structural and magnetic hybrid of cubic  $\text{CeIn}_3$  and quasi-2D  $\text{CeRhIn}_5$  that becomes a superconductor with  $T_c = 2.0$  K under applied pressure. It provides a previously unavailable example of structure-property relationships necessary for a more complete understanding of both the anomalous normal state and magnetically mediated superconductivity in strongly correlated f-electron materials.

PACS numbers: 74.70.Tx, 74.62.Fj, 75.30.Mb, 75.40.-s

Structure-property relationships can be helpful guides for developing new materials with desired functionalities as well as for developing an appropriate theoretical understanding of new properties. Structural layering of  $\text{CuO}_2$  sheets in the superconducting cuprates is a prominent example where these relationships have been particularly valuable. Relatively less attention has been given to structure-property relationships of f-electron compounds in which electronic correlations produce a quasiparticle mass  $m^*$  orders of magnitude larger than the mass of a free electron [1]. Of the nearly  $10^2$  examples of these heavy-fermion systems, there is no obvious correlation between their diverse structure types and the magnitude of the mass renormalization. This can be understood if the interaction primarily responsible for producing  $m^*$  is spatially local, for example the Kondo effect. However, unconventional superconductivity, which occurs in about 10% of the heavy-fermion compounds, appears dominantly in the tetragonal  $\text{ThCr}_2\text{Si}_2$  structure. With growing evidence that antiferromagnetic spin fluctuations mediate Cooper pairing in these unconventional superconductors [2, 3], this correlation suggests that the  $\text{ThCr}_2\text{Si}_2$  structure supports a fluctuation spectrum particularly favorable for superconductivity.

Recently, another structural family has been found that appears to favor heavy-fermion superconductivity.  $\text{CeCoIn}_5$  and  $\text{CeIrIn}_5$  crystallize in the  $\text{HoCoGa}_5$  structure and are heavy-fermion superconductors at atmospheric pressure with  $T_c$ 's of 2.3 and 0.4 K, respectively [4, 5]; while isostructural  $\text{CeRhIn}_5$  transforms from antiferromagnetic ( $T_N = 3.8$  K) at ambient pressure to superconducting ( $T_c = 2.1$  K) at a pressure of  $\sim 16$  kbar [6]. Unlike previous examples, these compounds are members of a larger family of structurally related materials with chemical compositions  $\text{Ce}_n\text{MIn}_{3n+2}$  with  $\text{M} = \text{Co}$ ,  $\text{Rh}$ ,  $\text{Ir}$  and  $n = 1, 2, \infty$ . The  $n = 1$  (2) members can be viewed crystallographically as one (two) layer(s) of  $\text{CeIn}_3$  separated by a single layer of ' $\text{MIn}_2$ ', a sequence repeated along the tetragonal c-axis. Besides  $\text{CeRhIn}_5$ ,  $\text{CeIn}_3$  and  $\text{Ce}_2\text{RhIn}_8$  are heavy-fermion antiferromagnets at ambient pressure. The  $n = \infty$  member, cubic  $\text{CeIn}_3$ , has a Néel temperature of 10 K and an ordered moment  $\mu_0 = 0.4$  to  $0.6\mu_B$  with propagation

wavevector  $Q = (\frac{1}{2}, \frac{1}{2}, \frac{1}{2})$  [7]. Applying hydrostatic pressure drives  $T_N$  to zero-temperature at a critical pressure  $P_c \approx 25$  kbar, and in the vicinity of  $P_c$ , superconductivity appears below 0.2 K [3]. Structural layering reduces  $T_N$  in  $\text{CeRhIn}_5$  and creates an incommensurate antiferromagnetic structure with  $Q = (\frac{1}{2}, \frac{1}{2}, 0.297)$  and  $\mu_0 = 0.37\mu_B$  [8]. The two-layer member  $\text{Ce}_2\text{RhIn}_8$  undergoes two magnetic transitions, one at  $T_N = 2.8$  K to a commensurate antiferromagnetic state with  $Q = (\frac{1}{2}, \frac{1}{2}, 0)$  and  $\mu_0 = 0.55\mu_B$  very similar to  $\text{CeIn}_3$  [9], and a second transition at  $T_{LN} = 1.65$  K to an incommensurate antiferromagnetic state [10, 11]. Except for its lower magnetic transition temperature,  $\text{Ce}_2\text{RhIn}_8$  might be considered a magnetic hybrid of  $\text{CeIn}_3$  and  $\text{CeRhIn}_5$ , exhibiting both commensurate and incommensurate structures, an ordered (commensurate) moment comparable to that of  $\text{CeIn}_3$  but an  $m^*$  (as reflected in its Sommerfeld coefficient of specific heat  $\gamma \approx 400\text{mJ/molK}^2$ ) equal to that of  $\text{CeRhIn}_5$ . Because both  $\text{CeIn}_3$  and  $\text{CeRhIn}_5$  are pressure-induced superconductors, in which antiferromagnetic spin fluctuations mediate Cooper pairing [3, 6], the structure-magnetic property relationships in  $\text{Ce}_2\text{RhIn}_8$  suggest that it might be superconducting under pressure. In the following, we present results of our high-pressure study of  $\text{Ce}_2\text{RhIn}_8$  and show that its response to pressure also reflects behaviors found in both  $\text{CeIn}_3$  and  $\text{CeRhIn}_5$ .

$\text{Ce}_2\text{RhIn}_8$  single crystals were grown out of excess In-flux. X-ray diffraction on powdered crystals revealed single-phase material in the primitive tetragonal  $\text{Ho}_2\text{CoGa}_8$  structure with lattice parameters  $a = 4.665$  Å and  $c = 12.244$  Å at room temperature. There was no evidence for intergrowth of  $\text{CeRhIn}_5$ . Samples with typical dimensions of  $1.0 \times 0.5 \times 0.5$  mm<sup>3</sup> were carefully screened by electrical resistance and susceptibility measurements for free In that might be present in the crystals. Samples without any detectable (less than 0.01 vol%) free indium were used for the present pressure experiments. Resistance measurements were carried out by a standard four-probe ac-technique using a resistance bridge, where the current was applied in the  $(a, b)$ -plane of the sample. Measurements of the dc and ac susceptibility were performed in a Quantum Design SQUID and a home-

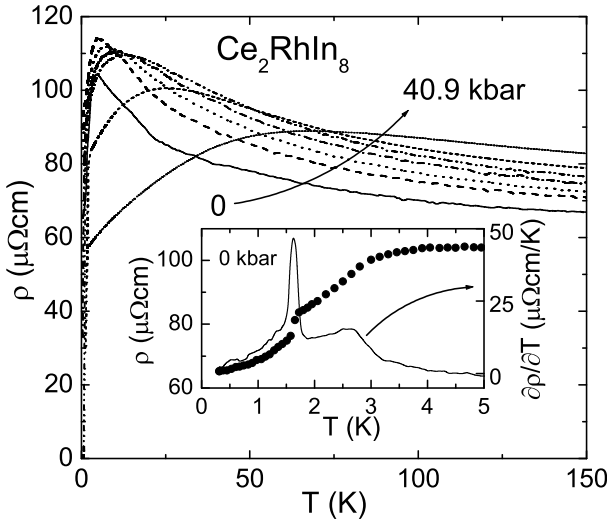


FIG. 1: Temperature dependence of the in-plane resistivity of  $\text{Ce}_2\text{RhIn}_8$  at various fixed pressures from ambient pressure up to 40.9 kbar. The inset shows the ambient pressure low-temperature resistivity and its derivative. The magnetic transitions are clearly indicated at  $T_N = 2.8$  K and  $T_{LN} = 1.65$  K, respectively.

made coil system, respectively. Three clamp-type cells were used to generate various fixed hydrostatic pressures up to 6 kbar for SQUID and 17 or 23 kbar for resistivity measurements. Flourinert-75 served as pressure medium. Hydrostatic pressures to 50 kbar were produced in a toroidal anvil cell using a glycerol-water mixture (3:2, volume ratio) [12]. In both types of cells, the superconducting transition of Pb (Sn), which served as a pressure gauge, remained sharp at all pressures, indicating a pressure gradient of less than 1-2% of the applied pressure.

The overall behavior of the resistivity is shown in fig. 1. The high temperature resistivity increases with increasing pressure over the temperature range between about 25 K and room-temperature. There is well-defined maximum in the resistivity at  $T_{\max} = 5$  K that initially decreases very weakly with  $P$  before beginning to increase above  $\sim 5$ -7 kbar. This unusual response is similar to that found in  $\text{CeRhIn}_5$  [6, 13]. For  $P > 20$  kbar,  $T_{\max}$  increases at a rate of  $\sim 2$  K/kbar. Compared to the typically small residual resistivity  $\rho_0$  of the  $\text{CeMIn}_5$  family members, for  $\text{CeRhIn}_5$  0.4  $\mu\Omega\text{cm}$  at 0.4 K [6],  $\rho_0$  for  $\text{Ce}_2\text{RhIn}_8$  is more than two orders of magnitude higher ( $\rho_0 \approx 65 \mu\Omega\text{cm}$ ), as is also the case for  $\text{Ce}_2\text{IrIn}_8$  [14]. This gives a residual resistivity ratio  $RRR \approx 1$  compared to 100 or even more for  $\text{CeMIn}_5$  [4, 5, 6] and  $\text{CeIn}_3$  [3]. The  $RRR$  is often used to give an estimate of sample quality and the influence of impurities/defects. There is no evidence for magnetic impurities from SQUID magnetometry, i.e., no impurity-derived Curie tail at low temperatures. This, combined with the sharp X-ray diffraction pattern, leads us to believe that a high residual resistiv-

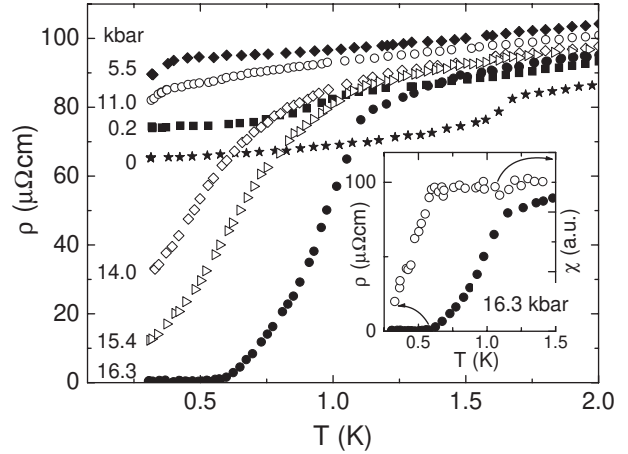


FIG. 2: Low-temperature resistivity of the in-plane resistivity of  $\text{Ce}_2\text{RhIn}_8$  at various fixed pressures. See text for details. With increasing pressure, a zero-resistivity and diamagnetic state evolves below 600 mK at 16.3 kbar as shown in the inset.

ity is intrinsic to the Ce218 compounds and may come from a slight out-of-plane buckling of In atoms at  $(\frac{1}{2}, \frac{1}{2}, 0.311)$ , which is not present in the Ce115 materials.

The low temperature resistivity and its derivative are shown in the inset of fig. 1. The lower magnetic transition is marked by a sharp peak in the derivative at  $T_{LN} = 1.65$ , which coincides with a sharp peak in specific heat measurements on the same crystal. The signature of the upper transition in the specific heat at  $T_{N,C_p} = 2.8$  K coincides with the inflection point in  $\partial\rho(T)/\partial T$ , rather than with the maximum. However, to define  $T_N$  at higher pressures, we use the maximum because the temperature at which there is an inflection point becomes poorly defined. This definition of  $T_N$  does not introduce a significant error in determining  $T_N(P)$ . At ambient pressure  $T_{N,\rho}$  is 2.65 K. Using this criterion and the data in fig. 1, we find that  $T_{N,\rho}$  decreases linearly at a rate  $\partial T_N/\partial P \approx -82$  mK/kbar. This initial slope was confirmed by dc susceptibility measurements to 5 kbar (open circles fig. 4). Although it was difficult to find a clear resistive signature for  $T_{N,\rho}$  at pressures greater than 7 kbar, a weak feature could be followed to 15 kbar, and this feature continued to move linearly to lower temperatures with increasing pressure (gray circles fig. 4). A linear extrapolation of these data to zero-temperature gives a critical pressure  $P_c \approx 30 \pm 5$  kbar. The initial slope and critical pressure of  $\text{Ce}_2\text{RhIn}_8$  are similar to those found for  $\text{CeIn}_3$ ,  $\partial T_N/\partial P \approx -60$  mK/kbar and 25 kbar, respectively [3]. These pressure dependencies contrast sharply with that of  $\text{CeRhIn}_5$  where  $T_N$  initially increases weakly with pressure [6].

We now focus on the response at lower temperatures. In contrast to  $T_N$ , the low-temperature magnetic transition is very sensitive to external pressure as shown in fig. 2. At 0.2 kbar  $T_{LN}$  shifts from 1.65 K at ambient

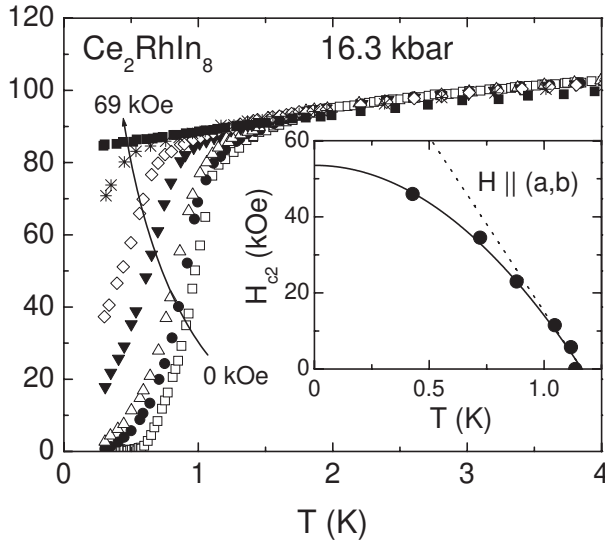


FIG. 3: Effect of a magnetic field on the resistivity of  $\text{Ce}_2\text{RhIn}_8$  at a pressure of 16.3 kbar and in various magnetic fields up to 69 kOe applied parallel to the tetragonal ( $a, b$ ) plane. The inset shows  $H_{c2}$  as a function of the temperature. The solid curve is a parabolic fit to  $(H_{c2}(T = 0) - H_{c2}(T))^2$  with  $H_{c2}(0) = 53.6$  kOe. The initial slope of  $H_{c2}(T)$  is indicated by the dashed line.

pressure to 0.95 K. This gives an estimate of a critical pressure  $P_{c,LN} \approx (0.4 \pm 0.1)$  kbar for suppressing  $T_{LN}$  and a corresponding slope of  $\partial T_{LN}/\partial P \approx -(4.3 \pm 1.5)$  K/kbar. This slope is consistent with  $\partial T_{LN}/\partial P$  derived from Ehrenfest's relation and measurements of the low-temperature specific heat and volume thermal expansion of  $\text{Ce}_2\text{RhIn}_8$  [11]. It appears that the incommensurate magnetic state is marginally stable. Specific heat measurements on many different crystals show [11] that some either do not have or exhibit a weak feature at  $T_{LN}$ , behavior invariably associated with a detectable amount of free In that may create internal stresses in the sample.

At 5.5 kbar a weak decrease in the resistivity appears at  $T_? = 420$  mK. Nearly the same temperature dependence of the resistivity and same  $T_?$  are found for 6.9 and 8.9 kbar (not shown). We note that the maximum in the resistivity at  $T_{\max}$  begins to increase when  $T_?$  first appears. At 11.0 kbar the data develop a steeper slope below  $\sim 1$  K followed by a kink near  $T_c = 380$  mK. The kink shifts continuously to higher temperatures with increasing pressure, accompanied by a dramatically reduced resistivity at the experimental base temperature, by 63% and 87% for 14.0 and 15.4 kbar, respectively, and finally a zero-resistance state appears below 595 mK at 16.3 kbar. Measurements of the ac susceptibility, plotted in the inset of fig. 2, show the onset of a diamagnetic response at the same temperature where the resistance goes to zero. Although perfect diamagnetism could not be observed in the experimentally accessible temperature range, it is clear from the size of the signal change

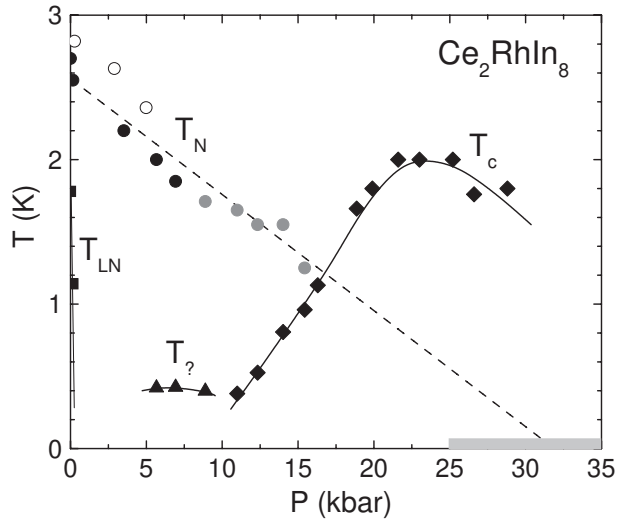


FIG. 4: The magnetic-superconducting phase diagram for  $\text{Ce}_2\text{RhIn}_8$  is shown in the  $P$ - $T$ -plane. The lines are guides to the eyes. The phase diagram is discussed in the text.

that the diamagnetic response is due to bulk superconductivity. Reproducibility of a zero-resistance state for  $P \geq 16$  kbar was confirmed on another crystal.

To provide additional confirmation of bulk superconductivity, we determined the upper critical field  $H_{c2}(T)$  at 16.3 kbar using data plotted in fig. 3. The resistive onset defines  $H_{c2}(T)$  which is shown in the inset. A fit of  $H_{c2} \propto (H_{c2}(T = 0) - H_{c2}(T))^2$  describes the data reasonably well with  $H_{c2}(0) = 53.6$  kOe and an initial slope  $-dH_{c2}/dT|_{T=T_c} = 91.8$  kOe/K [15]. The Ginzburg-Landau coherence length in the  $c$ -axis direction  $\xi_{GL} = [\frac{\Phi_0}{2\pi H_{c2}(0)}]^{0.5} \approx 77$  Å, which is about 6 times the  $c$ -axis lattice parameter. Assuming that  $H_{c2}(0)$  scales with  $T_c$ , these values are very comparable to those determined for  $\text{CeCoIn}_5$  [16] and  $\text{CeRhIn}_5$  at 25 kbar [13], which also exceed the Pauli paramagnetic limit. The dirty-limit relationship  $-dH_{c2}/dT|_{T=T_c} \propto \rho_0 \gamma$  [17] gives  $\gamma \approx 200$  mJ/moleCeK<sup>2</sup> at 16.3 kbar, which is one-half the value measured directly at atmospheric pressure just above  $T_N$ . Halving of the Sommerfeld coefficient at 16.3 kbar is expected from the relationship  $\gamma(P) \propto 1/T_{\max}(P)$  followed by several heavy-fermion systems and our observation that  $T_{\max}(16.3)/T_{\max}(0) = 2.5$  in  $\text{Ce}_2\text{RhIn}_8$ . This is strong evidence that the superconductivity arises in the bulk of  $\text{Ce}_2\text{RhIn}_8$ .

As shown by solid squares in fig. 3,  $\text{Ce}_2\text{RhIn}_8$  at 16.3 kbar and 69 kOe shows no evidence of a Fermi-like  $T^2$  dependence to its resistivity above 300 mK. A fit to these data finds  $\rho = \rho_0 + A'T^n$ , with  $n = 0.95 \pm 0.05$  for  $0.3 \text{ K} \leq T \leq 1.8 \text{ K}$ . This approximately  $T$ -linear resistivity is common to the Ce115 compounds [18] and distinct from the  $T^{1.6}$  non-Fermi liquid (NFL) behavior observed in  $\text{CeIn}_3$  near its critical pressure [3]. Although an approximately  $T^{\frac{3}{2}}$  temperature dependence is

expected [18] for a cubic material like  $\text{CeIn}_3$  near its antiferromagnetic quantum-critical point, an interpretation of the  $T$ -linear variation of the resistivity of  $\text{Ce}_2\text{RhIn}_8$  is less obvious. Various theoretical models [18] of quantum-critical behavior predict  $\rho \propto T$ , eg, for a 2D antiferromagnetic quantum critical point, but there is no evidence that  $\text{Ce}_2\text{RhIn}_8$  is strictly 2D. Within an antiferromagnetic spin-fluctuation scenario, strong electron scattering, implied by the high residual resistivity, would mix 'hot' and 'cold' regions of the Fermi surface and produce a temperature dependence stronger than linear [18]. This observation of a  $T$ -linear resistivity in  $\text{Ce}_2\text{RhIn}_8$  places additional constraints on its interpretation in the Ce115 materials since structurally and magnetically  $\text{Ce}_2\text{RhIn}_8$  is more 3D-like than the single layer compounds.

Additional measurements to 50 kbar, but for  $T \geq 1 \text{ K}$ , reveal that the onset temperature for superconductivity reaches a maximum of 2.0 K near 23 kbar before decreasing below 1 K above 35 kbar. Figure 4 shows the  $(P, T)$ -phase diagram up to 35 kbar.  $T_c$  reaches a maximum close to the pressure at which  $T_N$  extrapolates to zero. Unless  $T_N$  drops precipitously above  $\sim 15$  kbar, superconductivity and antiferromagnetism coexist over a substantial range of pressures. The linear decrease of  $T_N$  with pressure, a critical pressure of  $\sim 25$  kbar, and a maximum  $T_c$  near the extrapolated critical pressure are the responses of  $\text{CeIn}_3$  [3] and are distinctly different from the responses of  $\text{CeRhIn}_5$  to pressure [6, 13]. Further, the maximum  $T_c$  of  $\text{Ce}_2\text{RhIn}_8$  is very close to that of  $\text{CeRhIn}_5$  [13] but is an order of magnitude higher than in  $\text{CeIn}_3$ . Interestingly, the 'dome' of superconductivity exists over a rather broad pressure range, at least 25 kbar, in  $\text{Ce}_2\text{RhIn}_8$  but is very narrow,  $\sim 4$  kbar, in  $\text{CeIn}_3$ ; the pressure range over which superconductivity exists scales roughly with  $T_c$ .

As noted earlier, it is widely believed that spin fluctuations mediate pairing in the unconventional superconductivity of heavy-fermion materials [3]. From this work, we find that the commensurate antiferromagnetism and its pressure dependence in  $\text{Ce}_2\text{RhIn}_8$  are similar to that of the parent compound, cubic  $\text{CeIn}_3$ . One might expect, then, that the spin fluctuation spectrum of the two materials would be similar and, consequently, that both would have similar values of  $T_c$ . Contrary to this expectation,  $T_c$  is nearly as high as in the single layer compound  $\text{CeRhIn}_5$  and 10 times higher than in  $\text{CeIn}_3$ . A further distinction comes from the temperature dependence of the resistivity in the critical regime, approximately  $T$ -

linear in  $\text{Ce}_2\text{RhIn}_8$ , as in the  $\text{CeMIn}_5$  compounds, but approximately  $T^{\frac{3}{2}}$  in  $\text{CeIn}_3$ . Perhaps, this difference reflects differences in their respective spin fluctuation spectra that give rise to unconventional superconductivity. High-pressure inelastic neutron scattering would be valuable in resolving these issues. The unusual mixture of  $\text{CeIn}_3$ -like magnetism and  $\text{CeRhIn}_5$ -like superconductivity in  $\text{Ce}_2\text{RhIn}_8$  provides a heretofore unavailable example of structure-property relationships necessary for guiding a more complete understanding of unconventional superconductivity in strongly correlated electron systems.

We thank M. Hundley for screening several  $\text{Ce}_2\text{RhIn}_8$  samples. Work at Los Alamos was performed under the auspices of the US DOE.

---

\* Permanent address: Institute for High Pressure Physics, Russian Academy of Sciences, Troitsk, Russia.

† Permanent address: Departamento de Física, Pontifícia Universidade Católica do Rio de Janeiro, Brazil.

‡ Permanent address: Ames Laboratory, Ames, IA.

§ NHMFL, Florida State University, Tallahassee, FL.

- [1] Z. Fisk *et al.*, *Science*, **239**, 33 (1988); N. Grewe and F. Steglich, in *Handbook on the Chemistry and Physics of Rare Earths*, edited by K. A. Gschneidner and L. Eyring, Vol. 14 North-Holland, Amsterdam, 1991, p. 343.
- [2] N. K. Sato *et al.*, *Nature* **410**, 340 (2001).
- [3] N. D. Mathur *et al.*, *Nature* **394**, 39 (1998); G. Knebel *et al.*, *Phys. Rev. B* **65**, 024425 (2001).
- [4] C. Petrovic *et al.*, *Europhys. Lett.* **53** 354 (2001).
- [5] C. Petrovic *et al.*, *J. Phys.: Condens. Matter* **13** L337 (2001).
- [6] H. Hegger *et al.*, *Phys. Rev. Lett.* **84**, 4986 (2000).
- [7] J. M. Lawrence and S. M. Shapiro, *Phys. Rev. B* **22**, 4379 (1980); A. Benoit *et al.*, *Solid State Commun.* **34**, 293 (1980).
- [8] W. Bao *et al.*, *Phys. Rev. B* **62**, 14621(R) (2009); W. Bao *et al.*, *Phys. Rev. B* **63**, 219901(E) (2001).
- [9] W. Bao *et al.*, *Phys. Rev. B* **64**, 020401(R) (2001).
- [10] W. Bao, unpublished.
- [11] A. Malinowski *et al.*, unpublished.
- [12] V. A. Sidorov and O. B. Tsiok, *Fizika i Tekhnika Vysokikh Davlenii* **1**, 74 (1991).
- [13] T. Muramatsu *et al.*, *J. Phys. Soc. Jpn.* **70**, 3362 (2001).
- [14] M. Nicklas *et al.*, unpublished.
- [15] Similar measurements at 15.4 kbar give  $H_{c2}(0) = 44.8$  kOe and  $-\frac{dH_{c2}}{dT}|_{T=T_c} = 93.4$  kOe/K.
- [16] T. P. Murphy *et al.*, *Phys. Rev. B* **65**, 100514(R) (2002).
- [17] T. P. Orlando *et al.*, *Phys. Rev. B* **19**, 4545 (1979).
- [18] G. R. Stewart, *Rev. Mod. Phys.* **73**, 797 (2001).